

pubs.acs.org/biochemistry Communication

Regulation of Iron Homeostasis through Parkin-Mediated Lactoferrin Ubiquitylation

Ankur A. Gholkar, Stefan Schmollinger, Erick F. Velasquez, Yu-Chen Lo, Whitaker Cohn, Joseph Capri, Harish Dharmarajan, William J. Deardorff, Lucy W. Gao, Mai Abdusamad, Julian P. Whitelegge, and Jorge Z. Torres*



Cite This: https://dx.doi.org/10.1021/acs.biochem.0c00504



ACCESS

Metrics & More

Article Recommendations

s Supporting Information

ABSTRACT: Somatic mutations that perturb Parkin ubiquitin ligase activity and the misregulation of iron homeostasis have both been linked to Parkinson's disease. Lactotransferrin (LTF) is a member of the family of transferrin iron binding proteins that regulate iron homeostasis, and increased levels of LTF and its receptor have been observed in neurodegenerative disorders like Parkinson's disease. Here, we report that Parkin binds to LTF and ubiquitylates LTF to influence iron homeostasis. Parkindependent ubiquitylation of LTF occurred most often on lysines (K) 182 and 649. Substitution of K182 or K649 with alanine (K182A or K649A, respectively) led to a decrease in the level of LTF ubiquitylation, and substitution at both sites led to a major decrease in the level of LTF ubiquitylation. Importantly, Parkin-mediated ubiquitylation of LTF was critical for regulating intracellular iron levels as overexpression of LTF ubiquitylation site point mutants (K649A or K182A/K649A) led to an increase in intracellular iron levels measured by ICP-MS/MS. Consistently, RNAi-mediated depletion of Parkin led to an increase in intracellular iron levels in contrast to overexpression of Parkin that led to a decrease in intracellular iron levels. Together, these results indicate that Parkin binds to and ubiquitylates LTF to regulate intracellular iron levels. These results expand our understanding of the cellular processes that are perturbed when Parkin activity is disrupted and more broadly the mechanisms that contribute to Parkinson's disease.

Parkinson's disease (PD) is a debilitating neurodegenerative disease where it is ative disease whose incidence has increased over the past decade and presents a major public health epidemic. The PARK2 gene that encodes the Parkin E3 ubiquitin ligase is found to be mutated in familial forms of PD.2 Two pathological hallmarks of PD are the aggregation of α synuclein in Lewy bodies and the accumulation of iron.³ Lactotransferrin (lactoferrin or LTF) is a member of the family of transferrin iron binding proteins that transport iron and regulate intracellular iron levels. $^{4-6}$ X-ray structures of LTF show that it displays a bilobal architecture with one iron binding site within each lobe.^{7,8} Increased levels of LTF and its receptor have been reported within nigral neurons in PD patients and in other neurodegenerative disorders like Alzheimer's disease. 4,9-11 Iron homeostasis is important for maintaining the normal physiology of neuronal cell populations, and iron accumulation leads to neurotoxicity. 12 Due to this dysregulation of iron homeostasis during PD progression, iron chelators have been proposed as a potential therapeutic strategy. 13,14 Although many models for how iron-mediated cell death occurs in PD exist, most agree that an excess of reactive iron (Fe²⁺) leads to the generation of reactive oxygen species that induces oxidative stress and promotes neuronal cell death through toxic reactions that include mitochondrial dysfunction, lipid peroxidation, and protein misfolding. 13,14 Interestingly, transferrin (Tf)-containing endosomes have been shown to contact the mitochondria and may function to deliver iron directly to the mitochondria, 15 which could be a

mechanism that contributes to mitochondrial dysfunction. However, whether other members of the transferrin family, like LTF, function in a similar manner remains unclear. Although the dysregulation of Parkin and LTF had been previously linked to the accumulation of iron in populations of neuronal cells that undergo cell death in PD, a direct connection between the two had not been established.

To better understand the role of Parkin dysfunction in PD, we sought to identify novel Parkin ubiquitylation substrates. First, we established a HEK293 doxycycline-inducible localization and affinity purification (LAP = EGFP-TEV-S-Peptide)-tagged Parkin stable cell line and utilized it to express and tandem affinity-purified LAP-Parkin. 16,17 Eluates were analyzed by mass spectrometry to identify Parkin-associated proteins (Figure 1A). This analysis identified Parkin (270 peptides) and lactotransferrin (LTF, 72 peptides) as the most abundant proteins (Figure 1B and Table S1). Additionally, tubulin isoforms and proteasome subunits, known Parkininteracting proteins, 18-23 were also identified along with subunits of the CCT/TRiC complex (chaperonin-containing T-complex/TCP-1 ring complex), which is critical for tubulin

Received: June 16, 2020 Revised: July 22, 2020 Published: August 4, 2020



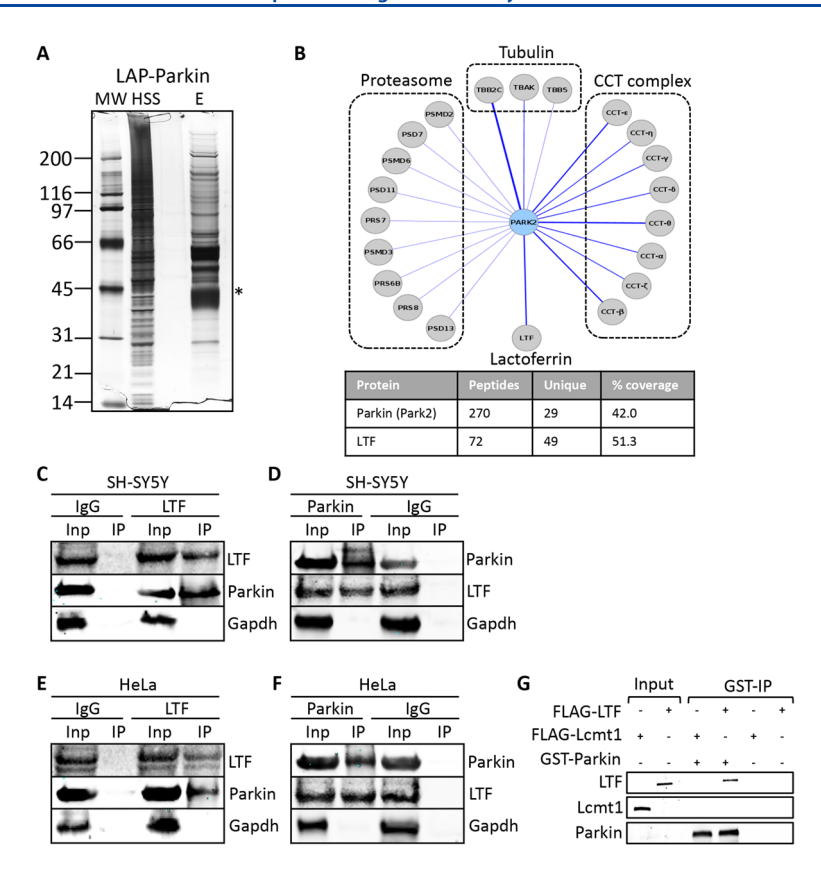


Figure 1. LTF co-purifies and associates with Parkin. (A) LAP—Parkin tandem affinity purification. Abbreviations: MW, molecular weight marker; HSS, high-spin supernatant; E, final eluates. The asterisk denotes the Parkin protein band. (B) Cytoscape visualization map of Parkin-associated proteins, identified by mass spectrometry, showing the major classes of co-purifying proteins. The bottom panel highlights the identification of lactoferrin (LTF) as a Parkin co-purifying protein. The protein name, the number of peptides identified, the number of unique peptides, and the percent protein coverage are indicated. See Table S1 for a complete list of Parkin co-purifying proteins identified by mass spectrometry. (C—F) SH-SYSY or HeLa cell extracts were used to perform reciprocal co-immunoprecipitation (Co-IP) experiments using anti-lactoferrin (LTF), anti-Parkin, and control IgG antibodies. Note that endogenous Parkin immunoprecipitates with endogenous LTF (C and E) and endogenous LTF immunoprecipitates with endogenous Parkin (D and F). Inp indicates input, and IP indicates immunoprecipitation. (G) In vitro binding assays performed in the presence or absence of in vitro-transcribed/translated FLAG—LTF, FLAG—Lcmt1, or GST—Parkin. GST—Parkin was immunoprecipitated (GST-IP), and eluates were analyzed by immunoblotting with the indicated antibodies. Note that FLAG—LTF immunoprecipitates with GST—Parkin, whereas control FLAG—Lcmt1 does not.

folding and for blocking the fibrillation of α-synuclein that is a pathological hallmark of PD (Figure 1B and Table S1).^{24–26} Due to the importance of LTF in iron homeostasis and its misregulation in PD,⁴ we sought to further validate the Parkin–LTF interaction. Reciprocal co-immunoprecipitation experiments from SH-SY5Y neuronal cells and HeLa cells with anti-Parkin and anti-LTF antibodies showed that LTF co-immunoprecipitated with Parkin and Parkin co-immunoprecipitated with LTF (Figure 1C–F). Similarly, *in vitro* protein binding reactions with GST-Parkin and FLAG–LTF showed that LTF co-immunoprecipitated with Parkin (Figure 1G). Together, these data indicated that LTF was associating with Parkin.

To understand the significance of Parkin–LTF association, we asked if LTF was ubiquitylated and whether its ubiquitylation was Parkin-dependent. LAP–LTF was immunoprecipitated from control siRNA (siCont) or Parkin siRNA (siParkin)-treated cells, and its ubiquitylation was monitored by immunoblot analysis with anti-ubiquitin antibodies. LAP–LTF was ubiquitylated in the siCont sample, and the level of this ubiquitylation was substantially decreased upon Parkin depletion with siParkin (Figure 2A). Next, we asked if LTF was a Parkin substrate using an *in vitro*-reconstituted

ubiquitylation assay. 27 GST-LTF, GST-tubulin (positive control), or GST-GFP (negative control) were incubated with an ATP regeneration system, ubiquitin, an E1 ubiquitinactivating enzyme, an E2 ubiquitin-conjugating enzyme, and wild-type (WT) or LAP-Parkin-overexpressing HEK293 cell extracts. Parkin substrate ubiquitylation was then monitored by immunoprecipitating the GST-tagged proteins and performing an immunoblot analysis with anti-ubiquitin and anti-GST antibodies. We observed ubiquitylation of GST-LTF and GST-tubulin (a known substrate of Parkin¹⁸) as a ladder of increasing molecular weight bands (Figure 2B). Next, we analyzed LTF ubiquitylation reactions by mass spectrometry and determined that LTF was ubiquitylated at seven different lysine (K) residues, with K182 and K649 being the most frequently modified sites (Table S2). Mapping of the ubiquitylation sites onto the human LTF crystal structure [Protein Data Bank (PDB) entry 1FCK] showed that all sites were on exposed loops (Figure 2C).

Next, we analyzed the contribution of the most frequently modified lysines (K182 or K649) to the overall ubiquitylation of LTF by substituting them with alanines and assessing LTF ubiquitylation. LAP-LTF-WT or LTF single (K182A or K649A) or double (K182A/K649A) ubiquitylation site point

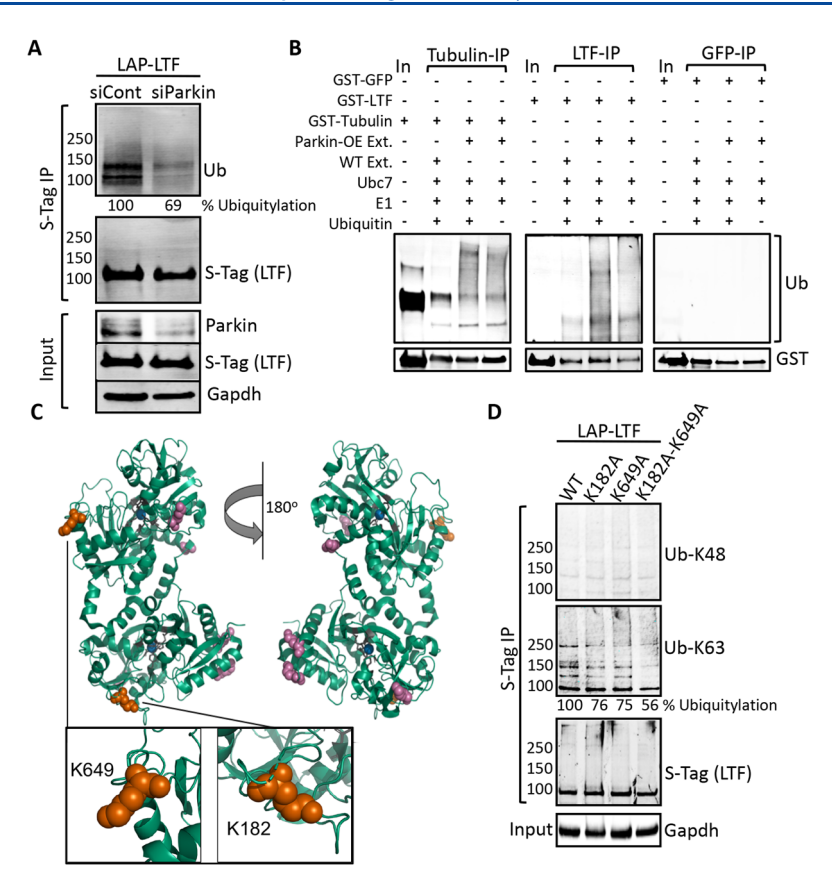


Figure 2. LTF is a substrate of Parkin. (A) Immunoblot analysis of LAP-LTF immunoprecipitated from HeLa cells treated with control nontargeting siRNA (siCont) or siRNA targeting Parkin (siParkin). Immunoprecipitation of LAP-LTF (S-Tag-IP) was monitored with anti-S-tag antibodies. LAP-LTF ubiquitylation was monitored with anti-ubiquitin antibodies (Ub). Depletion of Parkin was monitored with anti-Parkin antibodies, and anti-Gapdh antibodies were used as a control to monitor Gapdh protein levels. IP indicates immunoprecipitation. (B) In vitro ubiquitylation assays with or without recombinant GST-LTF, GST-tubulin (positive control), or GST-GFP (negative control); an ATP regeneration system; ubiquitin; E1 ubiquitin-activating enzyme; E2 ubiquitin-conjugating enzyme (Ubc7); and wild-type (WT) or LAP-Parkin-overexpressing (OE) HEK293 cell extracts (Ext). GST-tagged proteins were immunoprecipitated, and their ubiquitylation was monitored with anti-ubiquitin antibodies (Ub). IP indicates immunoprecipitation. (C) LTF ubiquitylation reactions were analyzed by mass spectrometry, and the most abundant Parkin-mediated LTF ubiquitylation sites, K182 and K649, were mapped onto the human LTF structure of PDB entry 1FCK (represented as orange spheres). Five additional ubiquitylation sites are represented as magenta spheres. Fe bound to LTF is represented as blue spheres. For a complete list of identified LTF ubiquitylation sites, see Table S2. (D) LAP-LTF-WT or LTF single (K182A or K649A) or double (K182A/K649A) ubiquitylation site mutants were expressed in HeLa cells and immunoprecipitated (S-Tag IP), and their ubiquitylation was monitored using anti-K48 and anti-K63 ubiquitin linkage specific antibodies. IP indicates immunoprecipitation.

mutants were expressed in HeLa cells and immunoprecipitated, and their ubiquitylation status was monitored using anti-K48 and anti-K63 ubiquitin linkage specific antibodies. K182A or K649A single mutants showed a reduction in the level of K63-linked ubiquitylation of LTF, and ubiquitylation of the LTF K182A/K649A double mutant was highly impaired compared to the WT control (Figure 2D). Together, these data indicated that LTF was a Parkin substrate and that K182A and K649A were the most frequently ubiquitylated sites and accounted for the majority of LTF-ubiquitylated species. Interestingly, LTF protein levels remained unchanged in HeLa or SH-SY5Y cells treated with Parkin siRNA or in Parkin knockout mice brains (Figure S1), indicating that Parkin did not regulate the levels of LTF.

Next, we sought to determine if ubiquitylation at K182 or K649 could influence the ability of LTF to regulate intracellular iron levels. Extracts from control HeLa cells or HeLa cells overexpressing the LTF wild type, K182A single mutant, K649A single mutant, or K182A/K649A double mutant were analyzed for intracellular sulfur (S), iron (Fe),

and zinc (Zn) levels using inductively coupled plasma mass spectrometry (ICP-MS/MS). For all ICP-MS/MS analyses, Fe and Zn levels were normalized to total S levels. Overexpression of the K649A variant alone or the K182A/K649A double mutant resulted in a similar significant increase in the intracellular Fe level compared to the control, while the Zn levels did not significantly change (Figure 3A,B). We hypothesized that if Parkin was ubiquitylating LTF on K649A to regulate iron levels, then modulation of Parkin levels would also affect intracellular iron levels. To test this, we performed RNAi-mediated depletion of Parkin levels and again analyzed the extracts for total S, Fe, and Zn. Decreasing Parkin levels led to a significant increase in Fe content compared to the control, while the Zn levels did not significantly change (Figure 4A,B). In contrast, extracts from cells that were overexpressing Parkin showed a significant decrease in total Fe levels compared to the control, while the Zn levels did not significantly change (Figure 4C,D). Together, these data demonstrated that Parkin abundance directly or the substitution of the Parkin-dependent LTF ubiquitylation site

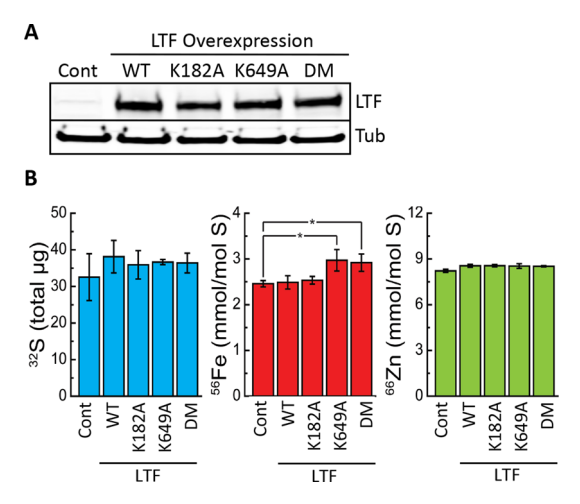


Figure 3. Overexpression of LTF ubiquitylation site mutants influences intracellular iron levels. (A) Extracts from control HeLa cells (Cont) or HeLa cells overexpressing the LAP–LTF wild type (WT), lysine 182 to alanine (K182A) point mutant, lysine 649 to alanine (K649A) point mutant, or double point mutant (K182A/K649A, indicated by DM) were analyzed for sulfur (32 S), iron (56 Fe), and zinc (66 Zn). (B) Total 32 S levels (in micrograms) were used to quantify 56 Fe and 66 Zn levels (in millimoles per mole of S). Bar graphs show the mean \pm standard deviation from three replicate samples. A t test was used to calculate p values (α < 5%) in the indicated comparisons.

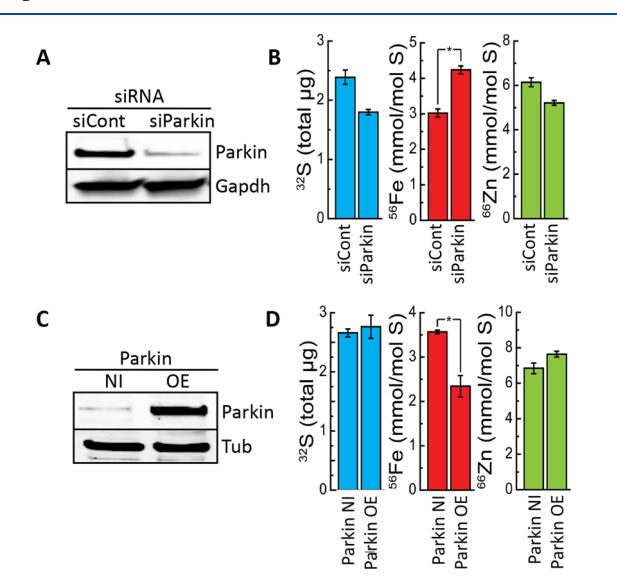


Figure 4. Parkin levels influence intracellular iron levels. (A and B) Extracts from HeLa cells transfected with control nontargeting siRNA (siCont) or Parkin siRNA (siParkin) were analyzed for total sulfur (32 S), iron (56 Fe), and zinc (66 Zn). (C and D) Extracts from the HEK293 LAP–Parkin-inducible cell line that was not induced (Parkin NI) or induced to overexpress LAP–Parkin (Parkin OE) were analyzed for total sulfur (32 S), iron (56 Fe), and zinc (66 Zn). NI indicates not induced, and OE indicates overexpression. (B and D) The total 32 S levels (in micrograms) were used to quantify 56 Fe and 66 Zn levels (in millimoles per mole of S). Bar graphs show the mean \pm standard deviation from three replicate samples. A t test was used to calculate p values (α < 5%) in the indicated comparisons.

(K649A) affects intracellular iron levels, consistent with a role for Parkin in regulating iron levels through LTF ubiquitylation. To begin to understand how Parkin-mediated ubiquitylation of LTF on K649 was affecting LTF metal binding, we performed

molecular dynamics simulations to compare the interaction potential energy in the LTF structure to the monoubiquitylated LTF structure. LTF structural studies have shown that the structure of LTF remains essentially the same irrespective of whether iron (Fe), cerium (Ce), or copper (Cu) is bound.²⁸⁻³¹ For this analysis, we used the structure of PDB entry 1FCK that is bound to Ce.³⁰ First, the monoubiquitylated LTF was modeled by conjugating the ubiquitin structure C-terminal glycine to K649 of human lactoferrin (see Materials and Methods) (Figure S2A). The molecular dynamics simulation showed that the monoubiquitylated LTF had an overall Ce binding stability that was lower than that of LTF with a mean initial interaction energy of approximately -2120kcal/mol compared to a value of -2170 kcal/mol. Furthermore, the stability of monoubiquitylated LTF decreased over the 100 ps simulation with an increased interaction energy while the Ce metal binding for LTF remained stable during the simulation (Figure S2B). Inspection of energy-minimized LTF and monoubiquitylated LTF structures revealed a shift in residues His597, Tyr435, and Arg465 that coordinate metal binding.²⁹ This in silico molecular analysis indicated that LTF ubiquitylation at K649 led to structural changes that destabilize metal coordination in the binding site and therefore could modulate metal (including iron) binding activity.

In summary, we have discovered a previously undescribed link between Parkin and LTF that influences iron homeostasis. We identified lactoferrin (LTF or lactotransferrin) as a Parkininteracting protein and validated this interaction through reciprocal co-immunoprecipitations from cells and in binding reactions in vitro. Increased levels of LTF and its receptor have been reported within nigral neurons in PD patients and in other neurodegenerative disorders. 4,9 Iron homeostasis is important for maintaining normal physiology of neuronal cell populations, and iron accumulation leads to neurotoxicity. 12 Due to the importance of LTF in iron homeostasis and its misregulation in PD, we sought to further define the significance of the Parkin-LTF interaction. We determined that LTF was ubiquitylated in a Parkin-dependent manner in cells and in vitro through K63 linkages. Moreover, we mapped the sites of seven lysines on the LTF lysine that were ubiquitylated, with K182 and K649 being the most abundantly modified. Substitution of K182 or K649 with an alanine (K182A or K649A) led to a decrease in the level of LTF ubiquitylation, and the double point mutant led to a major decrease in the level of LTF ubiquitylation. Importantly, Parkin-mediated ubiquitylation of LTF was critical for LTF's ability to modulate iron levels as overexpression of LTF ubiquitylation site point mutants K649A or K182A/K649A led to an increase in intracellular iron levels measured by ICP-MS/ MS. Consistently, RNAi-mediated depletion of Parkin also led to an increase in intracellular iron levels in contrast to overexpression of Parkin that led to a decrease in intracellular iron levels. Together, our data suggest that Parkin binds to and ubiquitylates LTF to influence intracellular iron levels. We propose that Parkin ubiquitylation of LTF at K649 perturbs LTF's ability to accumulate intracellular iron levels and that depletion of Parkin, or substitution of K649 on LTF, allows LTF to accumulate intracellular iron levels. The ability of Parkin to influence iron levels through LTF ubiquitylation may have direct implications for the increased iron levels that are observed in the nigral cells of PD patients. These results expand our understanding of the cellular processes that are

perturbed when Parkin activity is disrupted and more broadly the mechanisms that contribute to PD. LTF is a member of the family of transferrin iron binding proteins that transport iron and regulate intracellular iron levels. 4,5 It is currently unclear whether other isoforms of LTF like δ -lactoferrin³² or other transferrin iron binding proteins are regulated through ubiquitylation and whether their ubiquitylation is Parkinmediated. This study should help stimulate additional work related to Parkin-mediated iron regulation in PD and other neurological disorders. We note that the regulation of iron levels through Parkin-mediated ubiquitylation of LTF that we observe in vitro cannot solely account for the dysregulation in iron levels seen in PD patients and that other mechanisms are likely to exist. For example, the protein levels of divalent metal transporter 1 (DMT1), which transports metals, including iron, into the cell from the extracellular environment, have been shown to be regulated through Parkin-mediated ubiquitylation and proteasome-dependent degradation, and elevated levels of DMT1 have been observed in PD patients. 4,33,34 Furthermore, it is important to note that LTF can also influence the levels of other proteins with roles in iron homeostasis.³⁵ For example, studies analyzing the effect of bovine lactoferrin (bLf) on the inflammation response showed that the addition of exogenous bLf could inhibit iron overload by reducing the level of production of the pro-inflammatory cytokines IL-6 and IL-1 β and regulating iron metabolism through the upregulation of the iron exporter ferroportin (Fpn) and the transferrin receptor 1 (TfR1) and downregulation of ferritin (Ftn). 35,36 Thus, whether the changes in intracellular iron levels that we observe upon LTF ubiquitylation are directly related to LTF function or to the function of downstream iron-regulating proteins that are modulated by LTF remains to be determined.

ASSOCIATED CONTENT

Supporting Information

The Supporting Information is available free of charge at https://pubs.acs.org/doi/10.1021/acs.biochem.0c00504.

Tables, figures, and experimental methods (PDF)

Accession Codes

LTF, PO2788; Park2, 060260.

AUTHOR INFORMATION

Corresponding Author

Jorge Z. Torres — Department of Chemistry and Biochemistry, Jonsson Comprehensive Cancer Center, and Molecular Biology Institute, University of California, Los Angeles, California 90095, United States; orcid.org/0000-0002-2158-889X; Phone: 310-206-2092; Email: torres@chem.ucla.edu

Authors

Ankur A. Gholkar — Department of Chemistry and Biochemistry, University of California, Los Angeles, California 90095, United States

Stefan Schmollinger – Department of Chemistry and Biochemistry and Institute for Genomics and Proteomics, University of California, Los Angeles, California 90095, United States

Erick F. Velasquez — Department of Chemistry and Biochemistry, University of California, Los Angeles, California 90095, United States **Yu-Chen Lo** – Department of Chemistry and Biochemistry, University of California, Los Angeles, California 90095, United States

Whitaker Cohn — Pasarow Mass Spectrometry Laboratory, University of California, Los Angeles, California 90095, United States

Joseph Capri — Pasarow Mass Spectrometry Laboratory, University of California, Los Angeles, California 90095, United States

Harish Dharmarajan — Department of Chemistry and Biochemistry, University of California, Los Angeles, California 90095, United States

William J. Deardorff – Department of Chemistry and Biochemistry, University of California, Los Angeles, California 90095, United States

Lucy W. Gao — Pasarow Mass Spectrometry Laboratory, University of California, Los Angeles, California 90095, United States

Mai Abdusamad — Department of Chemistry and Biochemistry, University of California, Los Angeles, California 90095, United States

Julian P. Whitelegge — Pasarow Mass Spectrometry Laboratory, Jonsson Comprehensive Cancer Center, and Molecular Biology Institute, University of California, Los Angeles, California 90095, United States; ocid.org/0000-0003-2763-7733

Complete contact information is available at: https://pubs.acs.org/10.1021/acs.biochem.0c00504

Author Contributions

A.A.G. and J.Z.T. contributed to the design, execution, and analysis of experiments. M.A., H.D., and W.J.D. contributed to the experimentation. S.S. performed the ICP-MS/MS analyses. E.F.V. and Y.-C.L. performed LTF structure modeling. W.C., J.C., L.W.G., and J.P.W. performed mass spectrometry characterization of LTF ubiquitylation. A.A.G. and J.Z.T. wrote the final version of the manuscript.

Funding

This work was supported by National Science Foundation Grant NSF-MCB1912837 to J.Z.T., UCSD/UCLA NIDDK Diabetes Research Center Grant P30 DK063491 to J.P.W., U.S. Department of Energy Grant DE-FD02-04ER15529 to support S.S., a UCLA Molecular Biology Institute Whitcome Fellowship to E.F.V., and National Institutes of Health Grant GM42143 for instrument support.

Notes

The authors declare no competing financial interest.

ABBREVIATIONS

PD, Parkinson's disease; PARK2, Parkin; LTF, lactotransferrin; LAP, localization and affinity purification; ICP-MS/MS, inductively coupled plasma mass spectrometry.

REFERENCES

- (1) Connolly, B. S., and Lang, A. E. (2014) Pharmacological treatment of Parkinson disease: a review. *JAMA 311*, 1670–1683.
- (2) Panicker, N., Dawson, V. L., and Dawson, T. M. (2017) Activation mechanisms of the E3 ubiquitin ligase parkin. *Biochem. J.* 474, 3075–3086.
- (3) Lingor, P., Carboni, E., and Koch, J. C. (2017) Alpha-synuclein and iron: two keys unlocking Parkinson's disease. *J. Neural Transm* (Vienna) 124, 973–981.
- (4) Hirsch, E. C. (2009) Iron transport in Parkinson's disease. *Parkinsonism and Related Disorders* 15 (Suppl. 3), S209–S211.

- (5) Mazurier, J., Legrand, D., Hu, W. L., Montreuil, J., and Spik, G. (1989) Expression of human lactotransferrin receptors in phytohemagglutinin-stimulated human peripheral blood lymphocytes. Isolation of the receptors by antiligand-affinity chromatography. *Eur. J. Biochem.* 179, 481–487.
- (6) Qian, Z. M., and Wang, Q. (1998) Expression of iron transport proteins and excessive iron accumulation in the brain in neuro-degenerative disorders. *Brain Res. Rev.* 27, 257–267.
- (7) Thomassen, E. A., van Veen, H. A., van Berkel, P. H., Nuijens, J. H., and Abrahams, J. P. (2005) The protein structure of recombinant human lactoferrin produced in the milk of transgenic cows closely matches the structure of human milk-derived lactoferrin. *Transgenic Res.* 14, 397–405.
- (8) Andersen, B. F., Baker, H. M., Morris, G. E., Rumball, S. V., and Baker, E. N. (1990) Apolactoferrin structure demonstrates ligand-induced conformational change in transferrins. *Nature* 344, 784–787.
- (9) Faucheux, B. A., Herrero, M. T., Villares, J., Levy, R., Javoy-Agid, F., Obeso, J. A., Hauw, J. J., Agid, Y., and Hirsch, E. C. (1995) Autoradiographic localization and density of [1251]ferrotransferrin binding sites in the basal ganglia of control subjects, patients with Parkinson's disease and MPTP-lesioned monkeys. *Brain Res.* 691, 115–124
- (10) Leveugle, B., Faucheux, B. A., Bouras, C., Nillesse, N., Spik, G., Hirsch, E. C., Agid, Y., and Hof, P. R. (1996) Cellular distribution of the iron-binding protein lactotransferrin in the mesencephalon of Parkinson's disease cases. *Acta Neuropathol.* 91, 566–572.
- (11) Kawamata, T., Tooyama, I., Yamada, T., Walker, D. G., and McGeer, P. L. (1993) Lactotransferrin immunocytochemistry in Alzheimer and normal human brain. *Am. J. Pathol.* 142, 1574–1585.
- (12) Ward, R. J., Zucca, F. A., Duyn, J. H., Crichton, R. R., and Zecca, L. (2014) The role of iron in brain ageing and neuro-degenerative disorders. *Lancet Neurol.* 13, 1045–1060.
- (13) Weinreb, O., Mandel, S., Youdim, M. B. H., and Amit, T. (2013) Targeting dysregulation of brain iron homeostasis in Parkinson's disease by iron chelators. *Free Radical Biol. Med.* 62, 52–64.
- (14) Nunez, M. T., and Chana-Cuevas, P. (2019) New perspectives in iron chelation therapy for the treatment of Parkinson's disease. *Neural Regener. Res.* 14, 1905–1906.
- (15) Sheftel, A. D., Zhang, A. S., Brown, C., Shirihai, O. S., and Ponka, P. (2007) Direct interorganellar transfer of iron from endosome to mitochondrion. *Blood* 110, 125–132.
- (16) Torres, J. Z., Miller, J. J., and Jackson, P. K. (2009) High-throughput generation of tagged stable cell lines for proteomic analysis. *Proteomics 9*, 2888–2891.
- (17) Bradley, M., Ramirez, I., Cheung, K., Gholkar, A. A., and Torres, J. Z. (2016) Inducible LAP-tagged Stable Cell Lines for Investigating Protein Function, Spatiotemporal Localization and Protein Interaction Networks. *J. Visualized Exp. 118*, 54870.
- (18) Ren, Y., Zhao, J., and Feng, J. (2003) Parkin binds to alpha/beta tubulin and increases their ubiquitination and degradation. *J. Neurosci.* 23, 3316–3324.
- (19) Collins, G. A., and Goldberg, A. L. (2020) Proteins containing ubiquitin-like (Ubl) domains not only bind to 26S proteasomes but also induce their activation. *Proc. Natl. Acad. Sci. U. S. A. 117*, 4664–4674.
- (20) Upadhya, S. C., and Hegde, A. N. (2003) A potential proteasome-interacting motif within the ubiquitin-like domain of parkin and other proteins. *Trends Biochem. Sci.* 28, 280–283.
- (21) Sakata, E., Yamaguchi, Y., Kurimoto, E., Kikuchi, J., Yokoyama, S., Yamada, S., Kawahara, H., Yokosawa, H., Hattori, N., Mizuno, Y., Tanaka, K., and Kato, K. (2003) Parkin binds the Rpn10 subunit of 26S proteasomes through its ubiquitin-like domain. *EMBO Rep. 4*, 301–306.
- (22) Aguileta, M. A., Korac, J., Durcan, T. M., Trempe, J. F., Haber, M., Gehring, K., Elsasser, S., Waidmann, O., Fon, E. A., and Husnjak, K. (2015) The E3 ubiquitin ligase parkin is recruited to the 26 S proteasome via the proteasomal ubiquitin receptor Rpn13. *J. Biol. Chem.* 290, 7492–7505.

- (23) Safadi, S. S., and Shaw, G. S. (2010) Differential interaction of the E3 ligase parkin with the proteasomal subunit SSa and the endocytic protein Eps15. *J. Biol. Chem.* 285, 1424–1434.
- (24) Lundin, V. F., Leroux, M. R., and Stirling, P. C. (2010) Quality control of cytoskeletal proteins and human disease. *Trends Biochem. Sci.* 35, 288–297.
- (25) Sot, B., Rubio-Munoz, A., Leal-Quintero, A., Martinez-Sabando, J., Marcilla, M., Roodveldt, C., and Valpuesta, J. M. (2017) The chaperonin CCT inhibits assembly of alpha-synuclein amyloid fibrils by a specific, conformation-dependent interaction. *Sci. Rep.* 7, 40859.
- (26) Swinnen, E., Buttner, S., Outeiro, T. F., Galas, M. C., Madeo, F., Winderickx, J., and Franssens, V. (2011) Aggresome formation and segregation of inclusions influence toxicity of alpha-synuclein and synphilin-1 in yeast. *Biochem. Soc. Trans.* 39, 1476–1481.
- (27) Laney, J. D., and Hochstrasser, M. (2011) Analysis of protein ubiquitination. Curr. Protoc. Protein Sci. 66, 14.15.11–14.15.13.
- (28) Anderson, B. F., Baker, H. M., Dodson, E. J., Norris, G. E., Rumball, S. V., Waters, J. M., and Baker, E. N. (1987) Structure of human lactoferrin at 3.2-A resolution. *Proc. Natl. Acad. Sci. U. S. A.* 84, 1769–1773.
- (29) Baker, E. N., Anderson, B. F., Baker, H. M., Haridas, M., Jameson, G. B., Norris, G. E., Rumball, S. V., and Smith, C. A. (1991) Structure, function and flexibility of human lactoferrin. *Int. J. Biol. Macromol.* 13, 122–129.
- (30) Baker, H. M., Baker, C. J., Smith, C. A., and Baker, E. N. (2000) Metal substitution in transferrins: specific binding of cerium(IV) revealed by the crystal structure of cerium-substituted human lactoferrin. *JBIC*, *J. Biol. Inorg. Chem.* 5, 692–698.
- (31) Smith, C. A., Anderson, B. F., Baker, H. M., and Baker, E. N. (1992) Metal substitution in transferrins: the crystal structure of human copper-lactoferrin at 2.1-A resolution. *Biochemistry* 31, 4527–4533
- (32) Siebert, P. D., and Huang, B. C. (1997) Identification of an alternative form of human lactoferrin mRNA that is expressed differentially in normal tissues and tumor-derived cell lines. *Proc. Natl. Acad. Sci. U. S. A.* 94, 2198–2203.
- (33) Roth, J. A., Singleton, S., Feng, J., Garrick, M., and Paradkar, P. N. (2010) Parkin regulates metal transport via proteasomal degradation of the 1B isoforms of divalent metal transporter 1. *J. Neurochem.* 113, 454–464.
- (34) Salazar, J., Mena, N., Hunot, S., Prigent, A., Alvarez-Fischer, D., Arredondo, M., Duyckaerts, C., Sazdovitch, V., Zhao, L., Garrick, L. M., Nunez, M. T., Garrick, M. D., Raisman-Vozari, R., and Hirsch, E. C. (2008) Divalent metal transporter 1 (DMT1) contributes to neurodegeneration in animal models of Parkinson's disease. *Proc. Natl. Acad. Sci. U. S. A. 105*, 18578–18583.
- (35) Rosa, L., Cutone, A., Lepanto, M. S., Paesano, R., and Valenti, P. (2017) Lactoferrin: A Natural Glycoprotein Involved in Iron and Inflammatory Homeostasis. *Int. J. Mol. Sci.* 18, 1985.
- (36) Cutone, A., Rosa, L., Lepanto, M. S., Scotti, M. J., Berlutti, F., Bonaccorsi di Patti, M. C., Musci, G., and Valenti, P. (2017) Lactoferrin Efficiently Counteracts the Inflammation-Induced Changes of the Iron Homeostasis System in Macrophages. Front. Immunol. 8, 705.

SUPPORTING INFORMATION

Regulation of Iron Homeostasis Through Parkin-

mediated Lactoferrin Ubiquitylation

Ankur A. Gholkar¹, Stefan Schmollinger^{1,2}, Erick F. Velasquez¹, Yu-Chen Lo¹, Whitaker Cohn³,

Joseph Capri³, Harish Dharmarajan¹, William J. Deardorff¹, Lucy W. Gao³, Mai Abdusamad¹,

Julian P. Whitelegge^{3,4,5} and Jorge Z. Torres^{1,4,5*}

¹Department of Chemistry and Biochemistry, ² Institute for Genomics and Proteomics, ³Pasarow

Mass Spectrometry Laboratory, ⁴Jonsson Comprehensive Cancer Center, ⁵Molecular Biology

Institute, University of California, Los Angeles, CA 90095, USA

*Correspondence to:

Jorge Z. Torres

UCLA Department of Chemistry and Biochemistry

Los Angeles, CA 90095

Phone: 310-206-2092

torres@chem.ucla.edu

S1

Figures

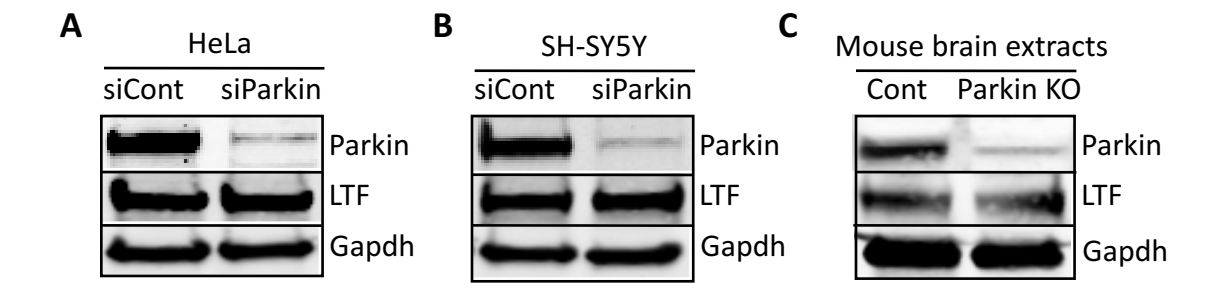


Figure S1. Depletion of Parkin does not alter LTF protein levels. (A-B) HeLa (A) or SH-SY5Y (B) cells were treated with control non-targeting siRNA (siCont) or siRNA targeting Parkin (siParkin) and extracts were immunoblotted with the indicated antibodies. Depletion of Parkin was monitored with anti-Parkin antibodies, LTF levels were monitored with anti-LTF antibodies, and anti-Gapdh antibodies were used as a control to monitor Gapdh protein levels. (C) Immunoblot analysis of control (Cont) and Parkin knock out (KO) mouse brain extracts with anti-Parkin, anti-LTF, and anti-Gapdh antibodies. (A-C) Note that LTF protein levels remain unchanged under all conditions.

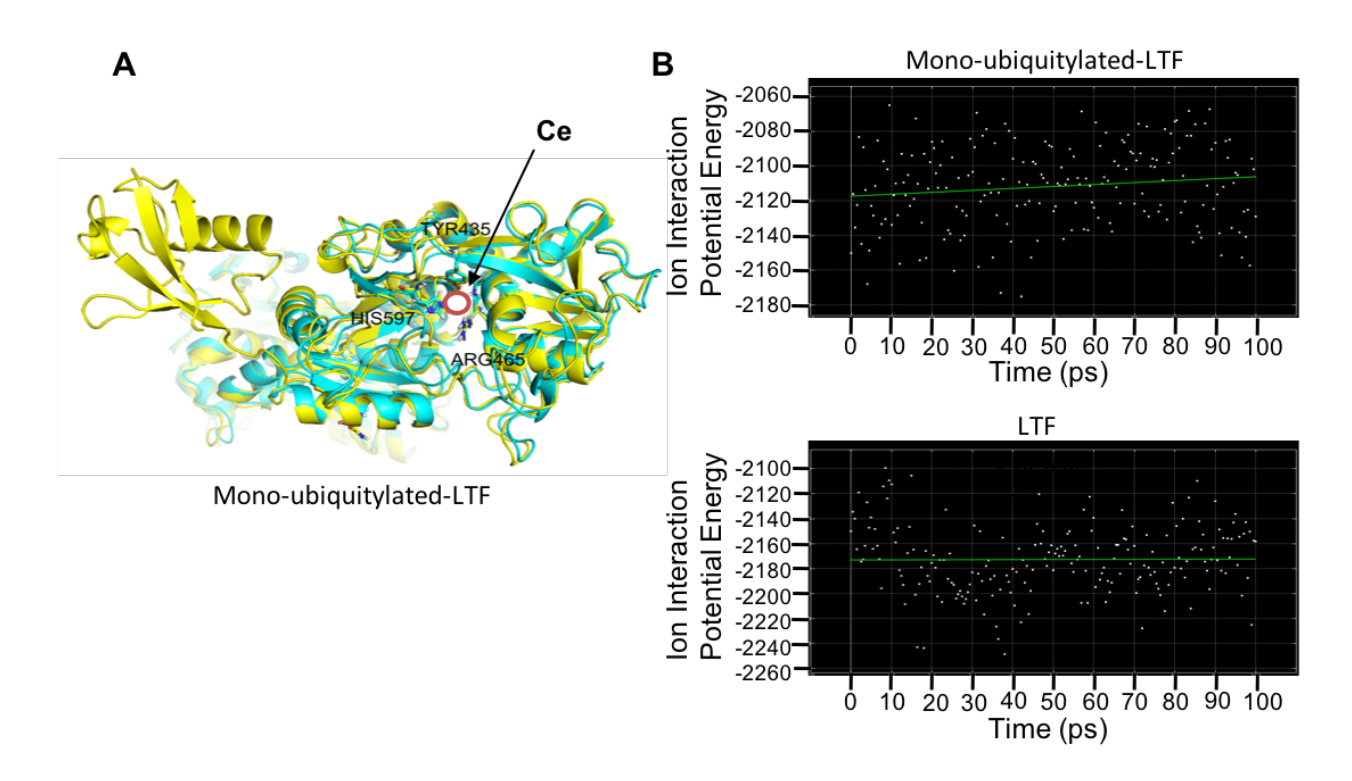


Figure S2. Molecular modeling and simulation of metal (cerium, Ce) binding to LTF and mono-ubiquitylated-LTF. (A) The mono-ubiquitylated-LTF (yellow) was modeled by conjugating the ubiquitin structure C-terminal glycine to Lysine 630 on the LTF structure (PDB: 1FCK) (corresponding to Lysine 649 on full-length LTF, see Materials and Methods). Inspection of energy minimized LTF and mono-ubiquitylated-LTF revealed a shift in the binding residues HIS597, TYR435, and ARG465 that coordinate the metal position (residue numbers correspond to residue numbers in the LTF PDB: 1FCK structure that is truncated compared to full-length LTF). (B) Molecular dynamics simulation of LTF and mono-ubiquitylated-LTF showed that the mono-ubiquitylated-LTF has an overall lower Ce binding stability than LTF with a mean initial interaction energy of ~-2120 kcal/mol compared to -2170 kcal/mol, respectively. Note that the stability of mono-ubiquitylated-LTF decreases over the 100 ps simulation with increased interaction energy while the Ce metal binding for LTF remains stable during the simulation. (x-axis: time in picoseconds, y-axis: interaction potential energy of Ce ion).

Materials and Methods

Cell culture. SH-SY5Y, HeLa, and HEK293 Flp-In T-REx LAP-tagged stable cell lines were grown in F12:DMEM 50:50 medium (GIBCO) with 10% FBS, 2 mM L-glutamine and antibiotics, in 5% CO₂ at 37°C. Cells were induced to express the indicated LAP-tagged proteins by addition of .1 μg/ml doxycycline (Sigma-Aldrich) for the indicated times.

Plasmids, mutagenesis, and generation of stable cell lines. Full length PARKIN or LTF cDNA was fused to the c-terminus of EGFP (pGLAP1 vector¹ or FLAG (pCS2-FLAG vector) as described previously². The LTF single (K182A and K649A) and double (K182A/K649A) mutants were generated using the QuickChange Lightning Site-Directed Mutagenesis Kit (Agilent Technologies) with primers carrying the desired mutations. All mutagenesis primers were purchased from Fisher Scientific, see **Table S3** for primer sequences. The pGLAP1-PARKIN, pGLAP1-LTF-K182A, pGLAP1-LTF-K649A, and pGLAP1-LTF-K182A/K649A vectors were used to generate doxycycline inducible HeLa Flp-In T-REx stable cell lines that express the fusion proteins from a specific single loci within the genome as described previously^{1,3}.

Cell extracts, immunoprecipitation and LAP purification. The indicted cell lines were harvested and cell extracts were prepared in LAP300 lysis buffer (50 mM Hepes pH 7.4, 300 mM KCl, 1 mM EGTA, 1 mM MgCl₂, 10% glycerol) plus 0.3% NP40, 0.5 mM DTT, 10 μM MG132, 20 mM NEM and protease and phosphatase inhibitor cocktail (Thermo Scientific). Immunoprecipitations were performed as described previously¹. Samples were resolved in a 4-20% gradient Tris gel (Bio-Rad) with TGS running buffer, transferred to PVDF membrane and

immunoblotted with indicated antibodies. Similarly LAP-tag tandem affinity purifications were performed as described previously¹. For mouse brain extract analyses, Parkin (Park2) knock out mice Park2^{tm1Shn}/Park2^{tm1Shn} (The Jackson Laboratory, cat#TSH0059, stock #006582) or control mice (The Jackson Laboratory, cat#TSH0058, stock #000664) brains were washed once with PBS and homogenized in the presence of RIPA buffer (150 mM NaCl, 1% IGEPAL CA-630, .5% sodium deoxycholate, .1% SDS, 50mM tris, pH 8.0) with protease and phosphatase inhibitor cocktail.

Identification of Parkin associated proteins by LC-MS/MS. HEK293 LAP-tag only or LAP-Parkin inducible stable cell lines were grown in roller bottles, induced with .1μg/ml Dox, harvested and lysed in the presence of protease (Roche), phosphatase (Pierce), and proteasome inhibitors (MG132, Enzo life sciences). LAP and LAP-Parkin were purified from extracts using a tandem affinity purification protocol¹. Eluates were resolved on a 4-12% SDS-PAG and ten gel slices corresponding to the resolved Parkin purification (and an adjacent control region) were excised and collected, washed twice with 50% acetonitrile, flash frozen, and stored until examination by mass spectrometry. Mass spectrometry-based proteomic analysis was performed at the Harvard Mass Spectrometry and Proteomics Resource Laboratory by microcapillary reverse-phase HPLC nano-electrospray tandem mass spectrometry (μLC/MS/MS) on a Thermo LTQ-Orbitrap mass spectrometer as described previously⁴. The major proteins identified in the LAP-Parkin but not in the LAP-tag only purification are listed in Table S1.

Quantitative metal and sulfur content analysis via ICP-MS/MS. The elemental content was analyzed as described previously⁵, with minor modifications to accommodate the sample

material. Briefly, HeLa cells (1×10^8) were collected by centrifugation at 1,500 rpm for 10 minutes. The cells were washed three times in 1 mM Na₂-EDTA (to remove cell surface associated metals and remnants from the growth media) and briefly once in Milli-Q water. The cell pellet, after removal of water, was overlaid with 286 µl 70% nitric acid (Fisher, Optima grade, A467-500, Lot 1216040) and digested at room temperature for 24 hours and at 65 °C for 4 hours, before being diluted to a final nitric acid concentration of 2% (v/v) with Milli-Q water. Iron, zinc and sulfur contents of the cell pellets were determined by inductively coupled plasma mass spectrometry (ICP-MS/MS) on an Agilent 8800 Triple Quadrupole ICP-MS instrument, in comparison to an environmental calibration standard (Agilent 5182-4688) and a sulfur standard (Inorganic Ventures CGS1), using 89Y as an internal standard (Inorganic Ventures MSY-100PPM). The levels of all analytes were determined in MS/MS mode by quantifying the most abundant isotope (32S, 56Fe and 66Zn); while 66Zn was measured directly using He in the collision/reaction cell, ⁵⁶Fe was directly determined using H₂ as a cell gas and ³²S was determined via mass-shift from 32 to 48, utilizing O₂ as a cell gas. The average of 4 technical replicate measurements was used for each individual sample or standard, the average variation in between the technical replicate measurements was 1.1% for all analytes and never exceeded 5% for any individual sample. Triplicate biological replicates were used to determine the variation in between samples, average and standard deviation between biological replicates are depicted in figures. Sulfur content was used to normalize for varying amount of cell material in between samples, since intracellular sulfur levels were unchanged in between the different samples.

Ubiquitylation reactions. Ubiquitylation reactions were carried out as described previously⁶. Briefly, GST-tagged LTF or positive control GST-tagged Tubulin or negative control GST-

tagged-GFP were incubated with or without HEK293 LAP-Parkin extracts, along with an ATP regeneration system, Ubiquitin, E1, and E2 in a buffer containing 20 mM HEPES, 5 mM NaCl, 5 mM MgCl2, DTT, MG132, protease and phosphatase inhibitor cocktail and incubated for 90 minutes at 30° C. GST beads were then added for 30 minutes, washed four times with a wash buffer containing 20 mM HEPES, 100 mM NaCl, 5 mM MgCl2, 15 mM imidazole, 0.5% TritonX, BME, DTT, MG132 and a protease and phosphatase inhibitor cocktail. The beads were then boiled in 2X Laemmli sample buffer (Bio-Rad) and loaded onto a 4-20% TGX gel (Bio-Rad) followed by western transfer. The blots were subsequently probed with anti-GST and anti-Ubiquitin antibodies.

siRNA treatments. Treatment of cells with ThermoFisher control non-targeting siRNA (12935300) and siRNAs previously shown to deplete PARKIN expression⁷ (1299001-HSS107594/HSS107593) was as described previously⁸.

Molecular modeling. To model LTF ubiquitylation, the C-terminal glycine residue of the ubiquitin structure (PDB: 1UBI) was conjugated to lysine 630 on the LTF structure (PDB: 1FCK), which corresponded to lysine 649 on full-length LTF, using the structure joining module with C-N bond length 1.54 A and dihedral angles of 180 degrees in the UCSF Chimera program (version 1.14)⁹. After removing the solvent molecules, both the LTF and mono-ubiquitylated-LTF models were subsequently protonated and energy minimized to stabilize structure RMS gradient to less than 0.1. To estimate the binding energy of bounded ion (Ce) to LTF and mono-ubiquitylated-LTF, we performed molecular dynamics simulation using NVT ensemble ¹⁰ at 300K by monitoring the interaction potential energy between ions and the receptors. The

molecular dynamics equation was performed for 100 ps under the light-bonded constraint and solved using the The Nosé-Poincaré-Anderson (NPA) method¹⁰. The molecular dynamics simulation was performed using the MOE software package (version 2009)¹¹. The models were visualized using the Pymol software package (version 1.8)¹².

Antibodies. See **Table S3** for a list of antibodies used for biochemical purifications, immunoprecipitations, and immunoblotting.

REFERENCES

- [1] Torres, J. Z., Miller, J. J., and Jackson, P. K. (2009) High-throughput generation of tagged stable cell lines for proteomic analysis, *Proteomics 9*, 2888-2891.
- [2] Torres, J. Z., Summers, M. K., Peterson, D., Brauer, M. J., Lee, J., Senese, S., Gholkar, A. A., Lo, Y. C., Lei, X., Jung, K., Anderson, D. C., Davis, D. P., Belmont, L., and Jackson, P. K. (2011) The STARD9/Kif16a Kinesin Associates with Mitotic Microtubules and Regulates Spindle Pole Assembly, *Cell* 147, 1309-1323.
- [3] Bradley, M., Ramirez, I., Cheung, K., Gholkar, A. A., and Torres, J. Z. (2016) Inducible LAP-tagged Stable Cell Lines for Investigating Protein Function, Spatiotemporal Localization and Protein Interaction Networks, *J Vis Exp* 118, 54870.
- [4] Vanderwerf, S. M., Svahn, J., Olson, S., Rathbun, R. K., Harrington, C., Yates, J., Keeble, W., Anderson, D. C., Anur, P., Pereira, N. F., Pilonetto, D. V., Pasquini, R., and Bagby, G. C. (2009) TLR8-dependent TNF-(alpha) overexpression in Fanconi anemia group C cells, *Blood 114*, 5290-5298.
- [5] Strenkert, D., Limso, C. A., Fatihi, A., Schmollinger, S., Basset, G. J., and Merchant, S. S. (2016) Genetically Programmed Changes in Photosynthetic Cofactor Metabolism in Copper-deficient Chlamydomonas, *J Biol Chem 291*, 19118-19131.
- [6] Gholkar, A. A., Senese, S., Lo, Y. C., Vides, E., Contreras, E., Hodara, E., Capri, J., Whitelegge, J. P., and Torres, J. Z. (2016) The X-Linked-Intellectual-Disability-Associated Ubiquitin Ligase Mid2 Interacts with Astrin and Regulates Astrin Levels to Promote Cell Division, *Cell Rep 14*, 180-188.
- [7] Muller-Rischart, A. K., Pilsl, A., Beaudette, P., Patra, M., Hadian, K., Funke, M., Peis, R., Deinlein, A., Schweimer, C., Kuhn, P. H., Lichtenthaler, S. F., Motori, E., Hrelia, S., Wurst, W., Trumbach, D., Langer, T., Krappmann, D., Dittmar, G., Tatzelt, J., and Winklhofer, K. F. (2013) The E3 ligase parkin maintains mitochondrial integrity by increasing linear ubiquitination of NEMO, *Mol Cell* 49, 908-921.
- [8] Torres, J. Z., Ban, K. H., and Jackson, P. K. (2010) A Specific Form of Phospho Protein Phosphatase 2 Regulates Anaphase-promoting Complex/Cyclosome Association with Spindle Poles, *Mol Biol Cell 21*, 897-904.

- [9] Pettersen, E. F., Goddard, T. D., Huang, C. C., Couch, G. S., Greenblatt, D. M., Meng, E. C., and Ferrin, T. E. (2004) UCSF Chimera--a visualization system for exploratory research and analysis, *J Comput Chem 25*, 1605-1612.
- [10] Frenkel, D., and Smit, B. (2002) *Understanding molecular simulation: from algorithms to applications*, Academic Press, San Doego, CA.
- [11] Vilar, S., Cozza, G., and Moro, S. (2008) Medicinal chemistry and the molecular operating environment (MOE): application of QSAR and molecular docking to drug discovery, *Curr Top Med Chem 8*, 1555-1572.
- [12] O'Donoghue, S. I., Goodsell, D. S., Frangakis, A. S., Jossinet, F., Laskowski, R. A., Nilges, M., Saibil, H. R., Schafferhans, A., Wade, R. C., Westhof, E., and Olson, A. J. (2010) Visualization of macromolecular structures, *Nat Methods* 7, S42-55.

Table S1. Summary of LC-MS/MS results from LAP-Parkin purifications

Swiss prot ID	Name	# of peptides	Unique	% coverage
Parkin				
O60260	Park2	270	27	46.9
Lactoferrin				
P02788	LTF	72	49	51.3
CCT Complex				
P17987	CCT-α	49	22	39.2
P78371	ССТ-В	74	24	39.7
P49368	ССТ-ү	49	24	35.8
P50991	CCT-δ	48	17	32.3
P02788	CCT-ε	71	25	35.1
P40227	CCT-ζ	46	19	28.5
Q99832	CCT-η	46	21	33.5
P50990	ССТ-Ө	82	29	48.6
Proteasome Co	mplex			
Q15008	PSMD6	6	6	17.2
P62195	PRS8	3	3	10.1
O00231	PSD11	2	2	5.5
P43686	PRS6B	2	2	3.8
P35998	PRS7	3	2	6
Q9UNM6	PSD13	2	2	5.3
O43242	PSMD3	3	3	5.8
Q13200	PSMD2	2	2	3
p51665	PSD7	1	1	3.7
Tubulins				
P68363	TBAK	41	12	25.7
P68371	TBB2C	111	17	38.4
P07437	TBB5	10	2	6.1
Ubiquitin				
P62988	Ubiquitin	22	4	61.8
Chaperones				
P07900	HSP90a	22	12	17.4
P08238	HSP90b	4	3	4.3
P11142	HSP70/HSP7	130	29	40.2
P08107	HSP70.1	3	1	1.7
Q27965	HSP70.2	73	19	27.3
P11021	HSP70/GRP7	16	12	22.6
P38646	HSP70/GRP7	11	7	12.5
P10809	HSP60	21	14	20.2
O95816	BAG2	9	6	25.6
P31689	DNJA1	12	7	19.1
O60884	DNJA2	12	7	16
Q9Y2Z0	SUGT1	3	3	11

Table S2. LTF Ubiquitylated Peptides

Analysis 1													
Query	Start	End	Observed	Mr(expt)	Mr(calc)	ppm	M	Score	Expect	Rank	Peptide	Peptides	LTF isoform 1 NP 002334.2
11691	119	139	597.5474	2386.1603	2386.2175	-24	2	6	6.4	10	K.KGGSFQLNELQGLKSCHTGLR.R + GlyGly (K)	1 of 11	NP_002334.2
11513	171	190	753.353	2257.0371	2257.0408	-1.67	1	7	0.77	1	R.FFSASCVPGADKGQFPNLCR.L + GlyGly (K)	2 of 2	K119
											, , , ,		K182
11514	171	190	753.3554	2257.0444	2257.0408	1.57	1	11	0.5	1	R.FFSASCVPGADKGQFPNLCR.L + GlyGly (K)	2 of 2	K 102
													K182
3340	292	299	525.2677	1048.5208	1048.5301	-8.86	1	3	2.9	7	R.QAQEKFGK.D + GlyGly (K)	1 of 1	K296
10237	300	315	932.989	1863.9635	1863.9479	8.35	2	8	2.6	7	K.DKSPKFQLFGSPSGQK.D + GlyGly (K)	1 of 1	. 200
													K305
11081	642	658	678.2952	2031.8637	2031.8666	-1.46	1	11	0.18	1	R.NGSDCPDKFCLFQSETK.N + GlyGly (K)	1 of 1	
													K649
A a b i a . 0													
Analysis 2 Query	Start	End	Observed	Mr(expt)	Mr(calc)	ppm	М	Score	Expect	Rank	Peptide	Peptides	LTF isoform 1
Quoi y	Otart		Obsci ved	WII (CXPI)	WIT(Calc)	ррпп	101	OCOIC	LAPOOL		replide	i optidos	NP_002334.2
9491	171	190	753.3558	2257.0455	2257.0408	2.06	1	1	1	2	R.FFSASCVPGADKGQFPNLCR.L + GlyGly (K)	4 of 4	
													K182
9493	171	190	753.358	2257.0523	2257.0408	5.06	1	10	0.83	1	R.FFSASCVPGADKGQFPNLCR.L + GlyGly (K)	4 of 4	
0404	474	100	752.2500	2257.0540	2257.0400	C 11	4	40	0.54		D FECASOVECADIVOCEDNII OD L. J. Olycly (IV)	4 - 4 4	K182
9494	171	190	753.3588	2257.0546	2257.0408	0.11	1	13	0.54	1	R.FFSASCVPGADKGQFPNLCR.L + GlyGly (K)	4 of 4	
9496	171	190	753.36	2257.0581	2257.0408	7.65	1	9	0.49	2	R.FFSASCVPGADKGQFPNLCR.L + GlyGly (K)	4 of 4	K182
8077	520	535	603.2715	1806.7928	1806.7876		0	16	0.49	1	R.SNLCALCIGDEQGENK.C + GlyGly (K)	1 of 1	K182 K535
9059	642	658	1016.944	2031.8735	2031.8666		1	18		1	R.NGSDCPDKFCLFQSETK.N + GlyGly (K)	3 of 3	K649
9060	642	658	678.2996	2031.8769	2031.8666		1	9	0.13	1	R.NGSDCPDKFCLFQSETK.N + GlyGly (K)	3 of 3	
9061	642	658	678.2997	2031.8774	2031.8666	5.31	1	15	0.084	1	R.NGSDCPDKFCLFQSETK.N + GlyGly (K)	3 of 3	K649
8110							-			•	, , , ,		K649
	695	709	905.9499	1809.8852	1809.8753	5.48	1	4	2.7	4	K.KCSTSPLLEACEFLR + GlvGlv (K)	1 of 3	VCOE
	695	709	905.9499	1809.8852	1809.8753	5.48	1	4	2.7	4	K.KCSTSPLLEACEFLR + GlyGly (K)	1 of 3	K695
Combined	695	709	905.9499	1809.8852	1809.8753	5.48	1	4	2.7	4	K.KCSTSPLLEACEFLR + GlyGly (K)	1 of 3	K695
Combined	695	709	905.9499	1809.8852	1809.8753	5.48	1	4	2.7	4	K.KCSTSPLLEACEFLR + GlyGly (K) K.KGGSFQLNELQGLKSCHTGLR.R + GlyGly (K)	1 of 3 1 of 11	K695
Combined	695	709	905.9499	1809.8852	1809.8753	5.48	1	4	2.7	4			
Combined	695	709	905.9499	1809.8852	1809.8753	5.48	1	4	2.7	4	K.KGGSFQLNELQGLKSCHTGLR.R + GlyGly (K)	1 of 11	K119
Combined	695	709	905.9499	1809.8852	1809.8753	5.48	1	4	2.7	4	K.KGGSFQLNELQGLKSCHTGLR.R + GlyGly (K) R.FFSASCVPGADKGQFPNLCR.L + GlyGly (K)	1 of 11 6 of 6	K119 K182
Combined	695	709	905.9499	1809.8852	1809.8753	5.48	1	4	2.7	4	K.KGGSFQLNELQGLKSCHTGLR.R + GlyGly (K) R.FFSASCVPGADKGQFPNLCR.L + GlyGly (K) R.QAQEKFGK.D + GlyGly (K)	1 of 11 6 of 6 1 of 1	K119 K182 K296
Combined	695	709	905.9499	1809.8852	1809.8753	5.48	1	4	2.7	4	K.KGGSFQLNELQGLKSCHTGLR.R + GlyGly (K) R.FFSASCVPGADKGQFPNLCR.L + GlyGly (K) R.QAQEKFGK.D + GlyGly (K) K.DKSPKFQLFGSPSGQK.D + GlyGly (K)	1 of 11 6 of 6 1 of 1 1 of 1	K119 K182 K296 K305
Combined	695	709	905.9499	1809.8852	1809.8753	5.48	1	4	2.7	4	K.KGGSFQLNELQGLKSCHTGLR.R + GlyGly (K) R.FFSASCVPGADKGQFPNLCR.L + GlyGly (K) R.QAQEKFGK.D + GlyGly (K) K.DKSPKFQLFGSPSGQK.D + GlyGly (K) R.SNLCALCIGDEQGENK.C + GlyGly (K)	1 of 11 6 of 6 1 of 1 1 of 1	K119 K182 K296 K305 K535

Table S3. Reagents Used

1. Primers

Name	Forward Primer	Reverse Primer	Company
LTF	5'GGGGACAAGTTTGTACAAAAAAG CAGGCTTCGAAGGAGATAGAACCA TGGGGAAACTTGTCTTCCTCGTCC TGC3'	5'GGGGACCACTTTGTACAAG AAAGCTGGGTCTCACTTCCTG AGGAATTCACAGGC3'	ThermoFisher
LTF (K182A)	5'CTGTGTTCCCGGTGCAGATGCAG GACAGTTCCCCAA3'	5'TTGGGGAACTGTCCTGCAT CTGCACCGGGAACACAG3'	ThermoFisher
LTF (K649A)	5'GACTGGAATAAGCAAAACGCGTC CGGGCAGTCAGATCC3'	5'GGATCTGACTGCCCGGACG CGTTTTGCTTATTCCAGTC3'	ThermoFisher
LTF (K182A- K649A)	Used K649A primers on LTF (K182A) mutant	Used K649A primers on LTF (K182A) mutant	ThermoFisher
Parkin	5'GGGGACAAGTTTGTACAAAAAAG CAGGCTTCGAAGGAGATAGAACCA TGGGGATAGTGTTTGTCAGGTTC3'	5'GGGGACCACTTTGTACAAG AAAGCTGGGTCCTACACGTC GAACCAGTG3'	ThermoFisher
LCMT-1	5'GGGGACAAGTTTGTACAAAAAAG CAGGCTTCGAAGGAGATAGAACCA TGGGGCTTCCCTGTGCAAGAGAAC TCC3'	5'GGGGACCACTTTGTACAAG AAAGCTGGGTCCTAATAAGTT ATCTCCTTCAGC3'	ThermoFisher

2. siRNA

Taget	siRNA ID	Catalog #	Company
Negative Control	N/A	12935300	ThermoFisher
PARK2	HSS107594	1299001	ThermoFisher
PARK2	HSS107593	1299001	ThermoFisher

3. Antibodies

Target	Name	Catalog #	Company
Ubquitin-K63	Ubquitin (linkage-specific K63) [EPR8590-448]	Ab179434	Abcam
Ubquitin-K48	Ubquitin (linkage-specific K48) [EP8589]	Ab140601	Abcam
LTF	Lactoferrin [2B8]	Ab10110	Abcam
Gapdh	Gapdh	GTX100118	GeneTex
Ubquitin	Mono- and polyubiquitinylated conjugates monoclonal antibody (FK2)	BML-PW8810-0100	Enzo
Parkin	Parkin	Ab15954	Abcam
Parkin	Parkin	#2132	Cell Signaling
S-Tag	S tag	GTX19321	GeneTex
GST	GST Tag (3G12B10)	66001-2-lg	Proteintech
IgG	normal rabbit lgG	12-370	Sigma Aldrich
lgG	normal mouse IgG	sc-2025	Santa Cruz

4. Proteins

Name	Details	Catalog #	Company
LTF	GST-Lactoferrin, Human	H00004057-P01-2ug	Novus
Tubulin	GST-Tubulin, Human	SRP5148-20UG	Sigma
Ubc7	His-UBE2G1 (UBC7), Human	009-001-U35S	Rockland
E1	His-E1, Human	BML-UW9410-0050	Enzo
Ubquitin	His-Ubiquitin, Human	BML-UW8610-0001	Enzo
GFP	GST-GFP	Torres Lab	Torres Lab

5. Affinity Resins

Name	Details	Catalog #	Company
Protein A Beads	Affi-Prep Protein A Media	156-0005	BIO-RAD
Protein G Beads	Pierce™ Protein G Magnetic Beads	88847	ThermoFisher
IGS L Beads	Pierce™ Glutathione Magnetic Agarose Beads	78601	ThermoFisher
S Beads	S-protein Agarose	69704-4	Millipore